

1 A note about density staircases in the Gulf of
2 Naples : 20 years of persistent weak salt-fingering
3 layers in a coastal area

4 Florian Kokoszka*, Daniele Iudicone*,
Adriana Zingone*, Vincenzo Saggiomo*,
Maurizio Ribera d'Alcalá*, and Fabio Conversano*

5 * *Stazione Zoologica Anton Dohrn, Naples, Italy*
6 Corresponding author: Florian Kokoszka
7 `florian.kokoszka@szn.it`

8 July 2021

9 Keywords

10 Coastal ecosystem, Mediterranean sea, time series, hydrological data, turbu-
11 lence, stratification, mixing, double-diffusion, salt-fingers

12
13 List of Figures

- 14 • Fig. 1 : Location and bathymetry of the Gulf of Naples in the Mediter-
15 ranean basin.
- 16 • Fig. 2 : Mean climatological seasonal cycle of the water-column occupa-
17 tion by the double-diffusive regime, and illustration of the density stair-
18 cases with an in-situ example.
- 19 • Fig. 3 : Time series (2001-2020) of the vertical profiles of the density ratio
20 and the parameterized effective eddy diffusivity.
- 21 • Fig. 4 : Statistical distributions and inter-annual variability of the salt-
22 fingering parameters.

23 Abstract

24 This is a short communication about the inter-annual recurring presence at the
25 coastal site in the Gulf of Naples of density staircases visible below the mixed
26 surface layer of the water-column, from the end of summer to the beginning of
27 winter, each year during nearly two decades of survey (2001 to 2020). We repet-
28 itively observe sequences from 1 to 4 small vertical staircases structures (~ 3 m
29 thick) in the density profiles ($\sim \Delta 0.2 \text{ kg m}^{-3}$), located between 10 m to 50 m
30 deep below the seasonal mixed layer depth. We interpret these vertical struc-
31 tures as the result of double diffusive processes that could host salt-fingering
32 regime (SF) due to warm salty water parcels overlying on relatively fresher
33 and colder layers. This common feature of the Mediterranean basin (i.e., the
34 thermohaline staircases of the Tyrrhenian sea) may sign here for the lateral
35 intrusions of nearshore water masses. These stably stratified layers are char-
36 acterized by density ratio R_ρ from 5.0 to 10.0, slightly higher than the critical
37 range ($1.0 - 3.0$) generally expected for fully developed salt-fingers. SF mixing,
38 such as parameterized (Zhang et al. (1998)), appears to inhibit weakly the ef-
39 fective eddy diffusivity with negative averaged value ($\sim -1 \times 10^{-8} \text{ m}^2 \text{ s}^{-1}$). A
40 quasi 5-year cycle is visible in the inter-annual variability of $\langle K^{\text{SF}} \rangle$, suggest-
41 ing a decadal modulation of the parameters regulating the SF regime. Even
42 contributing weakly to the turbulent mixing of the area, we hypothesize that
43 SF could influence the seasonal stratification by intensifying the density of deep
44 layers. Downward transfer of salt could have an impact on the nutrient supply
45 for the biological communities, that remains to be determined.

1 Introduction

Double diffusive mixing in the ocean is driven by the difference between molecular diffusivities of heat and salt (Stommel et al., 1956), the diffusion of heat being roughly 100 times faster than for salt (Zhang et al., 1998). This can be illustrated by the case of relatively warm water parcels that stabilize locally the water-column, tending to rapidly diffuse their heat content, while the slower diffusion of the salty content renders the vertical stability prompt to gravitational collapse. This situation leads to a transfer of salt toward the bottom, denominated as salt-fingering (SF) after their famously known chimney structure (Stommel et al., 1956; Stern, 1960; Linden, 1973). Another situation can occur too, when relatively cold and fresh water overlays on warmer and saltier parcels. Thermal content diffusion tends to stabilize upward, bringing salty parcels toward the surface, and an oscillatory diffusive (DDF) instability is generated. Once established in the water-column, these diffusive regimes can be identified in the vertical profiles of density by a series of well-mixed layers, whose staircases signature can extend from relatively vertical thin or fine-scale layers (e.g., 5 to 100-m thick intrusions, Ruddick, Richards (2003)) to larger structures (e.g. 300-m thick in the Tyrrhenian sea in Durante et al. (2019)). This process has been widely observed since decades in the ocean (e.g., Schmitt et al. (2005) in the Atlantic Ocean, Timmermans et al. (2003) and Lenn et al. (2009) in the Arctic), and particularly in the Mediterranean sea (Meccia et al., 2016; Falco, 2016), but field observations and time series acquisition remain of importance to investigate properly the temporal variability associated to these diffusive phenomenons, as pointed out by the study of Durante et al. (2019). Weak turbulent environment remains a key condition for their establishment against strong mixing processes (Timmermans et al., 2003), but the compilation of all in-situ observations demonstrates decades of their persistence in the Mediterranean basin with spatially distributed coherent patterns (Buffett et al., 2017). Even their turbulent mixing has been shown to contribute weakly to the ocean circulation (Lenn et al., 2009; Boog et al., 2021), their influence to the buoyancy flux can be significant in non-sheared environment and should be taken in account properly in the water-column budgets (Inoue et al., 2007). Due to the direct transfer of salt they provide toward the deep layers, and even weakly turbulent, double diffusive processes are effective and of importance to supply nutrients for the biological activity in the internal part of the water column (Fernández Castro et al., 2015)). Historically, studies of this phenomenon focused on the open and interior part of the ocean basins, but lakes, shallow seas and coastal area can be concerned too (Carniel et al., 2008; Schmid et al., 2010; Umlauf et al., 2018). Coastal marine ecosystem such as the Gulf of Naples is a mid-latitude semi-enclosed shallow basin in the Western Mediterrean Sea having a subtropical regime and almost no tides (**Fig. 1**). The area presents a marked salinity contrast due to the combination of the salty Tyrrhenian Sea waters, with its own feature of inshore/offshore water exchange with the open ocean, located on its southern side (Cianelli et al., 2015), and the freshwater inputs from a densely inhabited coastal area, on its northern part and from

91 nearby rivers (Cianelli et al., 2012, 2017).

92 The recent study of Kokoszka et al. (2021) in this location shows weak tur-
93 bulent observations during the seasonal destratification, associated to the pres-
94 ence of double-diffusive layers below the intrusion of warm salty layers present
95 in sub-surface from late summer to early winter. We extend this half-year pe-
96 riod analysis to the long-term time series in the Gulf of Naples with the use of
97 temperature and salinity profiles. These observations were made in the frame-
98 work of the Long Term Ecosystem Research Marechiaro (LTER-MC) initiative
99 that produced a historical time series of the mediterranean coastal ecosystem
100 of the Gulf of Naples through a weekly sampling of the water column started in
101 1984 and running until now (Ribera d'Alcala et al., 2004; Zingone et al., 2019).
102 We will focus here on the two last decades (January 2001 to March 2020), and
103 identify the layers of the water-column prompt to salt-finger regimes, to show
104 their variability, and estimate the associated eddy diffusivity, to determine their
105 possible contribution to the vertical mixing in such coastal area.

2 Materials and Methods

General hydrology

Conductivity–Temperature–Depth (CTD) profiles were carried out at the LTER-MC sampling point in the Gulf of Naples (**Fig. 1**) with a Seabird SBE-911+ mounted on a 12-bottle carousel, with all sensors calibrated. The raw profiles were processed using the Seabird data processing software to obtain 1-m bin-averaged data. The weekly survey refers to the casts MC465 (January 2001) to MC1359 (February 2020) and includes a total of 895 CTD profiles. The Gibbs-SeaWater Oceanographic Toolbox (McDougall, Barker, 2011) was used to calculate the conservative temperature Θ ($^{\circ}\text{C}$), the absolute salinity A_S (g kg^{-1}), the potential density σ_0 (kg m^{-3}), and the potential temperature θ_0 ($^{\circ}\text{C}$). When mentioned thereafter, temperature T and salinity S refer to Θ and A_S . Mixed layer depth (MLD, m) was calculated following the method of Boyer Montégut et al. (2004) based on threshold values. Given a vertical profile of density $\sigma_0(z)$, we calculated the depth below $z_{\text{ref}} = 3\text{m}$ where the profile reached a threshold defined as a cumulative of 0.03 kg m^{-3} .

Turner’s stability regimes

To produce reliable statistics of the double diffusive regimes, we followed the recommendation of Inoue et al. (2007) that compared successfully CTD estimates and dedicated turbulence measurements. We applied the same 10-m-scale averaging on temperature and salinity profiles, and conserved only the parts of the water column where the threshold for the minimum temperature gradient was $|\partial\bar{\theta}/\partial z| > 0.05 \text{ }^{\circ}\text{C m}^{-1}$ (Zhang et al., 1998; Inoue et al., 2007). This was shown to improve the statistics by embedding the information contained in the layer, that determines then the processes occurring at finer scales (Inoue et al., 2007). We applied the method introduced by Turner (Turner, 1967; 1973) to localize parts of the water column where vertical gradients of T and S are favourable to double-diffusive instability. Combining the vertical gradients and their signs allows the identification of stability regimes, that can be defined from the density ratio $R_\rho = (\alpha\partial\theta/\partial z)/(\beta\partial S/\partial z)$ where $\alpha = -\rho^{-1}(\partial\rho/\partial\theta)$ is the thermal expansion coefficient, $\beta = \rho^{-1}(\partial\rho/\partial S)$ is the haline contraction coefficient, where $\partial\rho/\partial z$ and $\partial\theta/\partial z$ are the vertical gradients of density and temperature, respectively. This ratio is used to calculate the Turner angles ($^{\circ}$) $Tu = \arctan((1 + R_\rho)/(1 - R_\rho))$ (Ruddick, 1983). The value of the Turner angle allows to identify various stability regimes. A diffusive convection regime (e.g., fresh cold layers over warm salty layer) arises when $-90^{\circ} < Tu < -45^{\circ}$. A double-diffusive regime (e.g., salty warm layer over cold fresh layer) arises when $45^{\circ} < Tu < 90^{\circ}$. Within each of these regimes, the instability is higher when $|Tu|$ is close to 90 degrees. A stable regime occurs when $|Tu| < 45^{\circ}$, whereas a gravitationally unstable regime occurs when $|Tu| > 90^{\circ}$. Generally, salt-fingering is considered active when $1 < R_\rho < 3$ (Inoue et al., 2007; Carniel

et al., 2008), but as illustrated thereafter on the **Fig. 2**, our observations exhibit small density staircases (~ 3 m) associated to slightly larger values of R_ρ (3.0 – 5.0), that should sign for a weak salt-fingering regime, but marked by persisting structures, visible repetitively weeks after weeks. Given that values $1 < R_\rho < 10$ are frequently observed (Kelley, 1990), and the large variability of the worldwide observations (You, 2002; Nakano, Yoshida, 2019), we included then all the cases $1 < R_\rho < 30$.

Salt-fingering diffusivities and salty flux

From the estimates of R_ρ , diffusivities of heat, salt, and density associated with salt-fingering have been extensively reviewed and are still discussed until now (Kunze, 2003; Nakano, Yoshida, 2019). Once identified parts of the water column prompt to SF regime, we apply the parameterization of Zhang et al. (1998) to obtain the effective salt and thermal diffusivities, respectively $K_S^{\text{SF}} = K^*/(1 + (R_\rho/R_C)^n)$ and $K_T^{\text{SF}} = \gamma^{\text{SF}}(K_S^{\text{SF}})/R_\rho$, where $n = 6$, $R_C = 1.6$, $K^* = 1 \times 10^{-4} \text{ m}^2 \text{ s}^{-1}$ a upper limit for the SF diffusivity, and γ^{SF} is computed as $\gamma^{\text{SF}} = 2.709e^{-2.512R_\rho} + 0.5128$ (Radko, Smith, 2012). Finally, we infer the effective eddy diffusivity of the density, $K_\rho^{\text{SF}} = (K_T^{\text{SF}} R_\rho - K_S^{\text{SF}})/(R_\rho - 1)$ (Eq. 8 in Nakano, Yoshida (2019)). As pointed out by the authors in their review, values of K_ρ^{SF} are negative, indicating that SF reduces the potential energy of the system by transferring salt downward in the water-column, and consequently intensifies density stratification. To illustrate that, we recall a general expression for the diffusivity (valid for heat, salt, or density) as a combination of salt-fingering (SF), double-diffusive (DDF), and other processes than double-diffusion (e.g., internal wave turbulence): $K^{\text{TOTAL}} = K^{\text{Turb.}} + K^{\text{SF}} + K^{\text{DDF}}$ (Merryfield et al., 1999; Merryfield, 2000; Inoue et al., 2007); K^{TOTAL} is generally dominated by the contribution of $K^{\text{Turb.}}$, and can be reduced by the negative values of K^{SF} . Please note that double-diffusive (DDF) will not be discussed in this work, and has been reviewed in detail by the mentioned authors. An estimate of buoyancy flux for salt is given by Kunze (1987) for SF developed on "thick" layers (> 1 m), as $g\beta F_S = 2\nu g\beta(\partial\bar{S}/\partial z)(R_\rho^{1/2} + (R_\rho - 1)^{1/2})^2$ (Kunze (1987), and Eq. 97 in Nakano, Yoshida (2019)), with g the gravitational acceleration (9.80 m s^{-2}), ν the kinematic molecular viscosity ($1.05 \times 10^{-6} \text{ m}^2 \text{ s}^{-1}$). Here F_S is the vertical salt flux ($\text{g kg}^{-1} \text{ m s}^{-1}$), βF_S the density flux of salt (m s^{-1}), and $g\beta F_S$ the buoyancy flux ($\text{m}^2 \text{ s}^{-3}$).

2.1 Results

Staircases layers during the seasonal cycle

Established from the weekly profiles of the whole period 2001-2020, the climatological monthly variations of salinity show a remarkable intrusion in subsurface (thick blue contour on **Fig. 2, top**), with values close to the maximum, between 38.05 and 38.1 g kg^{-1} , visible from September to November below 10 m depth, and above the 20 m to 45 m layer of relative less salty water ($< 38.0 \text{ g kg}^{-1}$). The thickness of this salty tongue increases in time following the deepening of the seasonal thermocline up to November (MLD in thick gray line on **Fig. 2, top**), progressively filling the water column, besides the first 5 m . Temperature (black contours on **Fig. 2, top**) shows a more classical seasonal cycle, with a mean maximum of around 26°C in July and August, decreasing to 20.0°C in September, then to 24.0°C and 18.0°C in October and November. From August to November these intrusions of salty water from 10 to 60 m create the unstable conditions for SF regime, whose water-column occupation is shown in plain blue on **Fig. 2 (top)**, below the MLD (thick gray).

The overview of the mean seasonal hydrological state allowed us to identify some general vertical distribution of SF regimes during the seasonal cycle. We illustrate this situation by showing a typical example of small staircases (e.g., during the cast MC1126 on **Fig. 2, bottom**). From around 25 to 45 m deep, both gradients of T and S are compatible with the host of SF regime. A sharp variation of nearly 0.2 g kg^{-1} is visible between 30 and 32 m , followed by a more moderate one of 0.1 g kg^{-1} from 32 to 37 m , associated both with a lost of temperature of nearly 1.0°C . The density profile is then marked by a sequence of thin and curvy staircases, progressing stably toward depth by steps of $\sim 0.20 \text{ kg m}^{-3}$ on vertical scales from 1 to 3 m . In terms of Turner angles, stronger value of 60° is obtained at 27 m where the instability presumably initiates from the salty and warm input, and progressively decreases to around 50° at 40 m where $T - S$ gradients stop to host the SF regime. Associated values of R_ρ vary from 3.0 to 5.0 where density staircases are the sharpest, then increase above 10.0 at the host ending. These values are slightly above the range in which SF are expected to be the most active ($1.0 - 3.0$), but density observations are marked by small curvy staircases, whose vertical structure have been smoothed by the 1-m scale vertical averaging of the data. Given these values of R_ρ and the shape of density profiles, we consider that we observe here a relatively weak SF regime, and this situation tends to repeat and persist in time during the season.

Unfolding the layers : nearly 20 years of staircase layers

This persistence during the two last decades is clearly demonstrated on the **Fig. 3** with the vertical distribution of R_ρ showing the vertical hosting of the SF regime below the mean MLD (gray line), mainly from August to November. Even being weak in general (Tu in the range $45 - 60^\circ$), the most intense

223 Turner angles values are more frequent in October and November than during
 224 the summer (see the vertical patterns on **Fig. 3**, and the red to blue distribu-
 225 tions on **Fig. 4**). Mean values of R_ρ are between 5.0 and 10.0, and occurrences
 226 < 5.0 are more frequent in October and November. Estimates of salt and
 227 thermal diffusivities reach mean values centered around $1 \times 10^{-8} \text{ m}^2 \text{ s}^{-1}$ and
 228 $4 \times 10^{-9} \text{ m}^2 \text{ s}^{-1}$ during these months, while the intensity is weaker and close to
 229 $1 \times 10^{-11} \text{ m}^2 \text{ s}^{-1}$ in August. This marks a seasonal differentiation in our obser-
 230 vations, the post-summer period being prompter to host the more intense SF
 231 regimes. When estimating the effective eddy diffusivity for the density, values of
 232 K_ρ^{SF} are negative, indicating that SF reduces the potential energy of the system
 233 by transferring salt downward in the water-column. Mean contribution is low
 234 ($-3 \times 10^{-8} \text{ m}^2 \text{ s}^{-1}$), compared to the averaged turbulent diffusivity expected in
 235 such coastal system (from $1 \times 10^{-6} \text{ m}^2 \text{ s}^{-1}$ to $1 \times 10^{-4} \text{ m}^2 \text{ s}^{-1}$). The range of
 236 the associated buoyancy flux for salt is around $-6 \times 10^{-9} \text{ m}^2 \text{ s}^{-3}$ from Septem-
 237 ber to October (see the yellow, orange and blue distributions on **Fig. 4**), and
 238 is centered closer to $-1 \times 10^{-8} \text{ m}^2 \text{ s}^{-3}$ in August (red). Consequently SF mix-
 239 ing, such as parameterized, appears to inhibit weakly the turbulent mixing of
 240 the area ($K^{\text{TOTAL}} = K^{\text{Turb.}} + K^{\text{SF}} + K^{\text{DDF}}$), but increase the stability of the
 241 deep layers by intensifying the density stratification due to the transfer of salt
 242 toward the bottom. The inter-annual values (black plots on **Fig. 4**) of K_ρ
 243 confirms these averages ranging from $-1 \times 10^{-10} \text{ m}^2 \text{ s}^{-1}$ to $-1 \times 10^{-6} \text{ m}^2 \text{ s}^{-1}$,
 244 and the low averaged buoyancy flux for salt ($\sim -6 \times 10^{-9} \text{ m}^2 \text{ s}^{-3}$) compared to
 245 the expected total buoyancy fluxes due to heat and freshwater by atmospheric
 246 forcings at the surface (of the order of $\sim 1 \times 10^{-7} \text{ m}^2 \text{ s}^{-3}$, see Kokoszka et al.
 247 (2021)). Noteworthy, a quasi 5-year cycle modulation is visible, affecting the
 248 transition of the first decade (2000-2009) to the second one (2010-2019), marked
 249 by weaker values for K_ρ . If these SF layers are the results of warm and salty
 250 intrusions, this suggest the presence of a climatic mechanism able to modulate
 251 the inter-annual variability inshore-offshore advection of such features at the
 252 time scale of the decade.

2.2 Discussion

The long-term monitoring (20 years) of the coastal station Marechiaro in the Gulf of Naples (LTER-MC, 75 m deep, 2 km off the coast) reveals noteworthy repetitive observations of small staircases vertical structures (~ 3 m) in the density field ($\sim \Delta 0.2 \text{ kg m}^{-3}$), whose presence is associated to surrounding layers of relatively warm and salty waters in sub-surface (from 10 to 50 m deep) from August to November, each year. We interpret these observations as the result of double-diffusive processes, i.e. here salt-fingering instabilities.

Such fine-scale structures may sign here for lateral intrusions (Merryfield, 2000; Umlauf et al., 2018), or interleaving (Ruddick, Richards, 2003; Ruddick, Kerr, 2003), whose inshore advection remains to be determined. These stably stratified layers are characterized by density ratio R_ρ from 5.0 to 10.0, close to some observations made in the Arctic Ocean (Timmermans et al., 2008; Shibley et al., 2017). As pointed out by Bebieva, Timmermans (2017), taking in account the horizontal gradients of T and S (intrusions), a critical value for the instability does not necessarily need to be close to 1.0, the higher values of R_ρ being the signature of T-S intrusions. This may be what we observe here, differing from the T-S staircases, typical of the neighbouring Tyrrhenian Sea (Zodiatis, Gasparini, 1996; Durante et al., 2019). In such configuration, dedicated parameterization taking account of horizontal gradients and using intermediate and higher R_ρ values should be investigated.

Given the averaged values of R_ρ (~ 5.0) and the observed values of turbulent mixing ($\langle K^{\text{Turb}} \rangle$ between 0.2 to $0.8 \times 10^{-5} \text{ m}^2 \text{ s}^{-1}$, in Kokoszka et al. (2021)), the inhibition due to negative $\langle K^{\text{SF}} \rangle$ in the *mixing mixture* (Inoue et al., 2007) is expected to be negligible, even some intermittent unstable occurrences (R_ρ close to 1.0) can be present in the SF layer below the MLD. Even mixing would be unaffected, the density stratification enforcement due to the transfer of salt could influence the generation and propagation of internal waves in such stratified-compatible layers (Kunze, 2003; Malki-Epshtein, Huppert, 2004; Maurer, Linden, 2014), followed then by their breaking in the deepest layers, more relaxed to the buoyancy-control of vertical motions. When the SF-compatible layers are located closer to the bottom (e.g., around 50 m in November), influence of boundary processes could be at work too, as suggested by the turbidity observations of Kokoszka et al. (2021). The step size of the observed structures could be a clue of the coexistence between weakly sheared internal wave and double-diffusion processes, as mentioned in the review of Kunze (2003). This feature of the shallow non-tidal area of the Gulf of Naples could provide an interesting in-situ experimental field to investigate and understand better the dynamic behind background gradients of tracers and velocity, and the growing of SF instabilities (Inoue et al., 2008; Ma, Peltier, 2021).

In general, implications for biological communities could be important. Compared to fluxes associated with mechanical forcings or mesoscale eddies, Oschlies et al. (2003) found the same magnitude attributed to double-diffusive processes, that showed a salt-finger driven enhancement of the upper ocean nutrient sup-

ply. As estimated in the work of Fernández Castro et al. (2015), nitrate diffusion mediated by salt fingers is responsible for $\sim 20\%$ of the new nitrogen supply in several areas of the Atlantic and Indian Oceans. More recently, Taillandier et al. (2020) showed that the nitrates supply across thermohaline staircases in the Western Mediterranean sea contributed at 25% to the budget of the Levantine intermediate water. The Gulf of Naples stands as a shallow bay connected to the open Tyrrhenian area, and Cianelli et al. (2017) shown here the importance of the interplay between coastal and offshore water masses to promote phytoplankton diversity. Their study identified the role of the horizontal mixing to enhance or dilute the favourable conditions for dominant species, and under this hypothesis we propose that salty intrusions (i.e., horizontal gradients), should be investigated in terms of their stability relative to the vertically surrounding layers. Given the downward transfer of salt due to SF regime in this shallow area where the photic layer prevails for the growing dynamic of the biological populations (Zingone et al., 1995, 2010), the importance of such a supply to the communities inhabiting the deep layers is a primer to determine. Because SF activity depends on the density ratio rather than on the stratification stability, its sensitivity to the future expected warming/freshening trends of the surface waters in the Mediterranean sea (Volosciuk et al., 2016) should be addressed, as shown by the inter-annual decadal variability already observable here at the coastal site in the Gulf of Naples.

Acknowledgments

Data sets for this research are available on request. We would like to thank the LTER-MC team that includes, besides the main authors: D. d’Alelio, C. Balestra, M. Cannavacciuolo, R. Casotti, I. Di Capua, F. Margiotta, M. G. Mazzocchi, M. Montresor, A. Passarelli, I. Percopo, M. Ribera d’Alcalà, M. Saggiomo, V. Saggiomo, D. Sarno, F. Tramontano, G. Zazo, A. Zingone, all based at the Stazione Zoologica Anton Dohrn of Naples. Special thanks must be given to A. Passarelli and the commandants and crews of the R/V Vettorica for all their dedicated work at sea. The research program LTER-MC is supported by the Stazione Zoologica Anton Dohrn.

References

- Bebieva Yana, Timmermans Mary-Louise. The Relationship between Double-Diffusive Intrusions and Staircases in the Arctic Ocean // Journal of Physical Oceanography. 02 2017. 47.
- Boog Carine, Dijkstra Henk, Pietrzak Julie, Katsman Caroline. Double-diffusive mixing makes a small contribution to the global ocean circulation // Communications Earth Environment. 02 2021. 2. 46.
- Boyer Montégut C. de, Madec G., Fischer A. S., Lazar A., Iudicone D. Mixed layer depth over the global ocean: An examination of profile data and profile-based climatology // Journal of Geophysical Research. 01 2004. 109. C12003.
- Buffett Grant George, Krahmann G., Klaeschen Dirk, Schroeder Katrin, Sallares Valenti, Papenberg Cord, R. Ranero Cesar, Zitellini Nevio. Seismic Oceanography in the Tyrrhenian Sea – Thermohaline Staircases, Eddies and Internal Waves // Journal of Geophysical Research: Oceans. 09 2017. 122.
- Carniel Sandro, Sclavo Mauro, Kantha Lakshmi, Prandke Hartmut. Double-diffusive layers in the Adriatic Sea // Geophysical Research Letters. 01 2008. 35.
- Cianelli Daniela, D’Alelio Domenico, Uttieri Marco, Sarno Diana, Zingone Adriana, Zambianchi Enrico, Ribera d’Alcala Maurizio. Disentangling physical and biological drivers of phytoplankton dynamics in a coastal system // Scientific Reports. 12 2017. 7.
- Cianelli Daniela, Falco Pierpaolo, Iermano Ilaria, Mozzillo Pasquale, Uttieri Marco, Buonocore B., Zambardino Giovanni, Zambianchi Enrico. In-shore/offshore water exchange in the Gulf of Naples // Journal of Marine Systems. 01 2015.
- Cianelli Daniela, Uttieri Marco, Buonocore B., Falco Pierpaolo, Zambardino Giovanni, Zambianchi Enrico. Dynamics of a very special Mediterranean coastal area: the Gulf of Naples // Mediterranean Ecosystems: Dynamics, Management and Conservation. 08 2012. 129–150.
- Durante Sara, Schroeder Katrin, Mazzei L., Pierini S., Borghini M., Sparnocchia S. Permanent Thermohaline Staircases in the Tyrrhenian Sea // Geophysical Research Letters. 01 2019.
- Falco Pierpaolo. Water mass structure and deep mixing processes in the Tyrrhenian Sea: Results from the VECTOR project // Deep Sea Research Part I Oceanographic Research Papers. 04 2016. 113.
- Fernández Castro Bieito, Mourino Beatriz, Maranon Emilio, Chouciño P, Gago J., Ramírez Teodoro, Vidal Montserrat, Bode Antonio, Blasco D, Royer

367 Sarah-Jeanne, Estrada Marta, Simó Rafel. Importance of salt fingering for
368 new nitrogen supply in the oligotrophic ocean // Nature communications. 09
369 2015. 6. 8002.

370 GEBCO Compilation Group. GEBCO 2020 Grid. 2020.

371 Inoue R., Kunze E., Laurent L., Schmitt Raymond, Toole John. Evaluating
372 salt-fingering theories // Journal of Marine Research. 07 2008. 66.

373 Inoue Ryuichiro, Yamazaki Hidekatsu, Wolk Fabian, Kono Tokihiro, Yoshida
374 Jiro. An Estimation of Buoyancy Flux for a Mixture of Turbulence and
375 Double Diffusion // Journal of Physical Oceanography. 03 2007. 37.

376 Kelley Dan. Fluxes Through Diffusive Staircases, A New Formulation // Journal
377 of Geophysical Research. 03 1990. 95. 3365–3371.

378 Kokoszka Florian, Conversano Fabio, Iudicone Daniele, Ferron Bruno,
379 Bouruet-Aubertot Pascale, Mc Millan Justine. Microstructure observations
380 of the summer-to-winter destratification at a coastal site in the Gulf of Naples
381 // Essoar pre-print. 7 2021.

382 Kunze Eric. Limits on Growing, Finite-Length Salt Fingers, A Richardson
383 Number Constraint // J. Mar. Res. 08 1987. 45. 533–556.

384 Kunze Eric. A review of oceanic salt-fingering theory // Progress In Oceanog-
385 raphy. 03 2003. 56. 399–417.

386 Lenn Yueng-Djern, Wiles P.J., Torres-Valdés Sinhué, Abrahamsen Einar,
387 Rippeth Tom, Simpson John, Bacon S., Laxon S., Polyakov I., Ivanov
388 Vladimir, Kirillov Sergey. Vertical mixing at intermediate depths in the Arctic
389 boundary current // Geophysical Research Letters. 03 2009. 36. L05601.

390 Linden P.F. On the Structure of Salt Fingers // Deep Sea Res. 04 1973. 20.
391 325–340.

392 Ma Yuchen, Peltier W. Gamma instability in an inhomogeneous environment
393 and salt-fingering staircase trapping: Determining the step size // Physical
394 Review Fluids. 03 2021. 6.

395 Malki-Epshtein Liora, Huppert Herbert. Internal waves and velocity scales of
396 double-diffusive intrusions // 57th Annual Meeting of the APS Division of
397 Fluid Dynamics, 21-23 November, 2004, Seattle, USA. 01 2004.

398 Maurer Benjamin, Linden P. Intrusion-generated waves in a linearly stratified
399 fluid // Journal of Fluid Mechanics. 08 2014. 752. 282–295.

400 McDougall T.J., Barker P.M. Getting started with TEOS-10 and the Gibbs
401 Seawater (GSW) Oceanographic Toolbox // SCOR/IAPSO WG. 2011. 127.
402 1—28.

403 Meccia Virna, Simoncelli Simona, Sparnocchia Stefania. Decadal variability of
404 the Turner Angle in the Mediterranean Sea and its implications for double
405 diffusion // Deep Sea Research Part I: Oceanographic Research Papers. 08
406 2016. 114. 64–77.

407 Merryfield William. Origin of Thermohaline Staircases // Journal of Physical
408 Oceanography - J PHYS OCEANOGR. 05 2000. 30. 1046–1068.

409 Merryfield William, Holloway Greg, Gargett Ann. A Global Ocean Model with
410 Double-Diffusive Mixing // Journal of Physical Oceanography - J PHYS
411 OCEANOGR. 06 1999. 29. 1124–1142.

412 Nakano Haruka, Yoshida Jiro. A note on estimating eddy diffusivity for oceanic
413 double-diffusive convection // Journal of Oceanography. 05 2019.

414 Oschlies Andreas, Dietze H., Kähler Paul. Salt-finger driven enhancement of
415 upper ocean nutrient supply // Geophysical Research Letters - GEOPHYS
416 RES LETT. 12 2003. 30.

417 Radko Timour, Smith D. Equilibrium transport in double-diffusive convection
418 // Journal of Fluid Mechanics. 01 2012. 692.

419 Ribera d'Alcala Maurizio, Conversano Fabio, Corato Federico, Licandro P.,
420 Mangoni Olga, Marino D., Mazzocchi Maria Grazia, Modigh M., Montresor
421 Marina, Nardella M., Saggiomo Vincenzo, Sarno Diana, Zingone Adriana.
422 Seasonal patterns in plankton communities in pluriannual time series at a
423 coastal Mediterranean site (Gulf of Naples): An attempt to discern recur-
424 rences and trends // Scientia Marina. 04 2004. 68. 65–83.

425 Ruddick B., Richards K. Oceanic thermohaline intrusions: Observations //
426 Progress In Oceanography. 03 2003. 56. 499–527.

427 Ruddick Barry. A Practical Indicator of the Stability of the Water Column
428 to Double-Diffusive Activity // Deep Sea Research Part A. Oceanographic
429 Research Papers. 10 1983. 30. 1105–1107.

430 Ruddick Barry, Kerr Oliver. Oceanic thermohaline intrusions: Theory //
431 Progress In Oceanography. 03 2003. 56. 483–497.

432 Schmid Martin, Busbridge Myles, Est Alfred. Double-diffusive convection in
433 Lake Kivu // Limnology and Oceanography. 01 2010. 55.

434 Schmitt Raymond, Ledwell J, Montgomery Ellyn, Polzin K, Toole John. En-
435 hanced Diapycnal Mixing by Salt Fingers in the Thermocline of the Tropical
436 Atlantic // Science (New York, N.Y.). 05 2005. 308. 685–8.

437 Shibley N., Timmermans M.-L, Carpenter J.R., Toole John. Spatial variability
438 of the Arctic Ocean's double-diffusive staircase // Journal of Geophysical
439 Research: Oceans. 02 2017. 122.

440 Stern Melvin. The “Salt-Fountain” and Thermohaline Convection // Tellus. 05
441 1960. 12. 172 – 175.

442 Stommel Henry, Arons Arnold, Blanchard Duncan. An Oceanographical Cu-
443 riosity, The Perpetual Salt Fountain // Deep Sea Res. 01 1956. 3. 152–153.

444 Taillandier Vincent, Prieur Louis, D’Ortenzio Fabrizio, Ribera d’Alcala
445 Maurizio, Pulido-Villena Elvira. Profiling float observation of thermohaline
446 staircases in the western Mediterranean Sea and impact on nutrient fluxes //
447 Biogeosciences. 07 2020. 17. 3343–3366.

448 Timmermans Mary-Louise, Garrett Chris, Carmack Eddy. The Thermohaline
449 Structure and Evolution of the Deep Water in the Canada Basin, Arctic Ocean
450 // Deep Sea Research Part I: Oceanographic Research Papers. 10 2003. 50.

451 Timmermans Mary-Louise, Toole John, Krishfield Richard, Winsor Peter. Ice-
452 Tethered Profiler observations of the double-diffusive staircase in the Canada
453 Basin thermocline // Journal of Geophysical Research. 12 2008. 113.

454 Turner J. Salt Fingers Across a Density Interface // Deep Sea Research and
455 Oceanographic Abstracts. 10 1967. 14. 599–611.

456 Buoyancy Effects in Fluids. // . 01 1973.

457 Umlauf Lars, Holtermann Peter, Gillner Christiane, Prien Ralf, Merckelbach
458 Lucas, Carpenter Jeffrey. Diffusive Convection under Rapidly Varying Con-
459 ditions // Journal of Physical Oceanography. 06 2018. 48.

460 Volosciuk C., Maraun D., Semenov V. A., Tilinina N., Gulev S. K., , Latif M.
461 Rising Mediterranean Sea Surface Temperatures Amplify Extreme Summer
462 Precipitation in Central Europe // Scientific Reports. 2016. 6, 32450.

463 You Yuzhu. A global ocean climatological atlas of the Turner angle: Implications
464 for double-diffusion and water-mass structure // Deep Sea Research Part I:
465 Oceanographic Research Papers. 11 2002. 49. 2075–2093.

466 Zhang Jubao, Schmitt Raymond, Huang Rui. Sensitivity of the GFDL Modular
467 Ocean Model to Parameterization of Double-Diffusive Processes // Journal
468 of Physical Oceanography - J PHYS OCEANOGR. 04 1998. 28. 589–605.

469 Zingone Adriana, Casotti Raffaella, Ribera d’Alcala Maurizio, Scardi Michele,
470 Marino Donato. St-Martin’s Summer - The case of an Autumn phytoplankton
471 bloom in the Gulf of Naples (Mediterranean-Sea) // Journal of Plankton
472 Research. 03 1995. 17. 575–593.

473 Zingone Adriana, D’Alelio Domenico, Mazzocchi Maria Grazia, Montresor
474 Marina, Sarno Diana. Time series and beyond: Multifaceted plankton re-
475 search at a marine Mediterranean LTER site // Nature Conservation. 05
476 2019. 34. 273–310.

- 477 Zingone Adriana, Dubroca Laurent, Iudicone Daniele, Margiotta Francesca,
478 Corato Federico, Ribera d'Alcala Maurizio, Saggiomo Vincenzo, Sarno Diana.
479 Coastal Phytoplankton Do Not Rest in Winter // Estuaries and Coasts. 03
480 2010. 33. 342–361.
- 481 Zodiatis George, Gasparini Gian. Thermohaline staircase formations in the
482 Tyrrhenian Sea // Deep-sea Research Part I-oceanographic Research Papers
483 - DEEP-SEA RES PT I-OCEANOGRAPHIC RES. 05 1996. 43. 655–678.

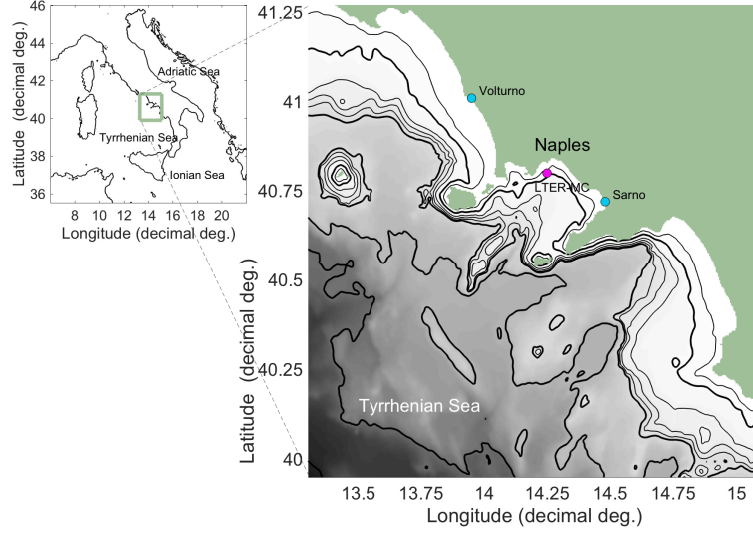


Figure 1: Bathymetry of the Gulf of Naples (GEBCO grid (GEBCO, 2020)) along the Tyrrhenian Sea in the Mediterranean basin). The 75m-deep LTER-MC coastal sampling site ($14.25^{\circ}E$, $40.80^{\circ}N$) is located by the pink dot. Volturno and Sarno's river mouths are shown in blue. Thin lines indicate the 50, 200, 300 and 400 m isobaths, thick ones indicate the 100, 500, 1000 and 2000 m isobaths.

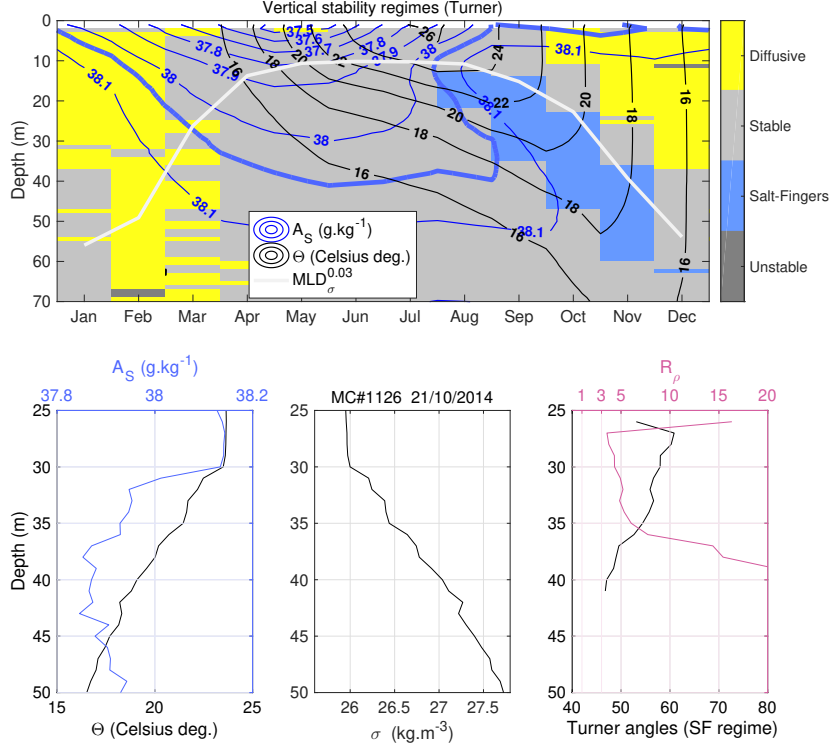


Figure 2: **Top** : Seasonal water-column occupation by the four stability regimes of Turner, showing vertical layers prompt to possibly host double-diffusive instabilities (SF or DDF), inferred from the monthly climatological profiles established with the weekly CTD data from 2001 to 2020 (MC465 to MC1359). Black and blue : contours of the climatological temperature and salinity profiles. Thick blue : 38.05 g.kg⁻¹ haline level, showing the salty intrusion. Light gray : seasonal mixed layer depth (MLD). **Bottom** : Illustration of a density staircase situation (cast MC1126). Left : temperature and salinity profiles ; Center : density ; Right : Turner angles and density ratio R_ρ (SF regime).

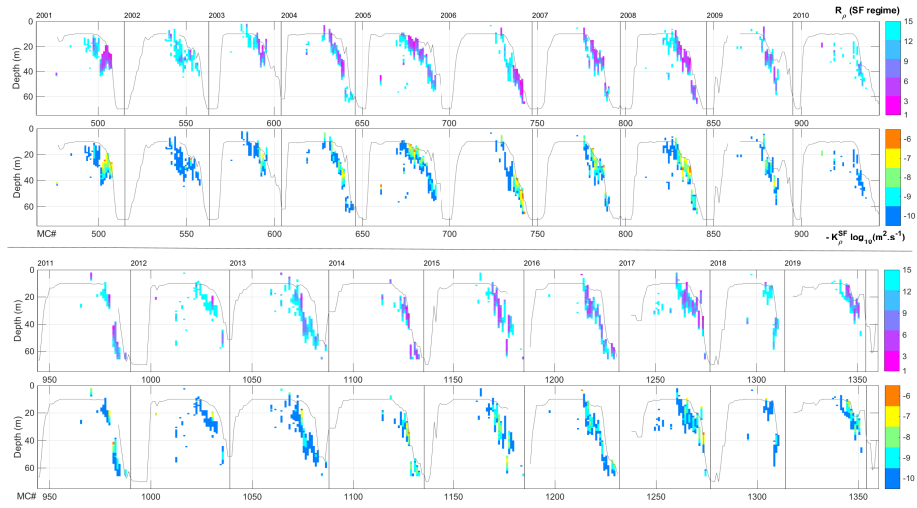


Figure 3: Time series of the vertical profiles of R_ρ (pink to light blue chart, on Top) and the effective eddy diffusivity K_ρ (blue to orange chart, on Bottom), for the SF regime. Decades are splitted between upper (2001-2010) and lower (2011-2020) panels. Y-axis indicates the depth of profiles, x-axis indicates the sequence of weekly MC casts (MC465 to MC1359). Years are indicated at the top. Gray line : mixed layer depth.

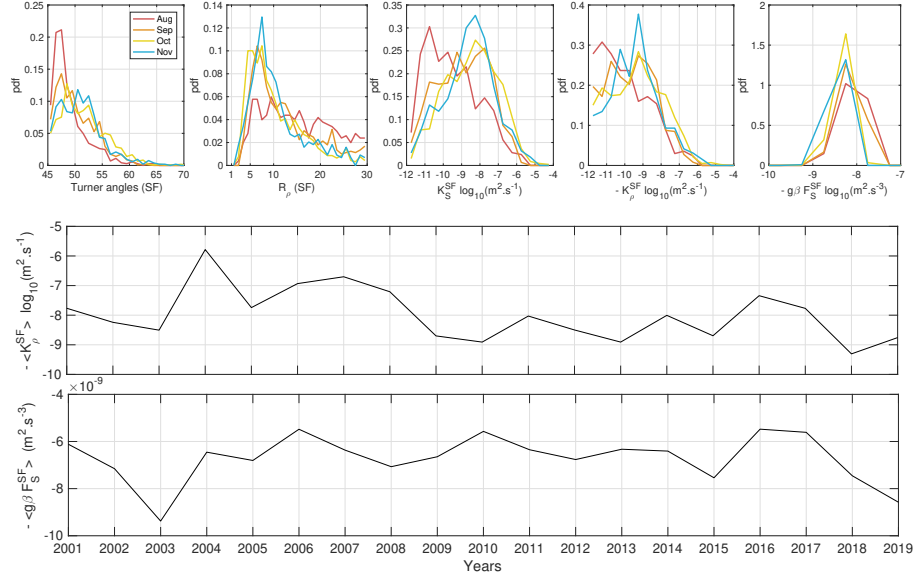


Figure 4: **Top** : Probability density function (PDF) associated with the following parameters in the SF regime : Turner angles, R_ρ , effective salt diffusivity (K_S), effective eddy diffusivity (K_ρ), and buoyancy flux for salt. Distributions have been established from the whole period available (2001 to 2020), and separated for the four month of August to November when SF regime is possible. **Bottom** : Inter-annual variability of the year-averaged mean values of K_ρ^{SF} and buoyancy flux for salt $g\beta F_S^{\text{SF}}$ (note the negative values).